AIMS Materials Science, 5(3): 508–518.
DOI: 10.3934/matersci.2018.3.508
Received: 24 October 2017
Accepted: 22 January 2018
Published: 25 May 2018

http://www.aimspress.com/journal/Materials

Communication

Nano bio-MOFs: Showing drugs storage property among their multifunctional properties

Tabinda Sattar and Muhammad Athar*

Institute of Chemical Sciences, BZU, Multan, Pakistan

*** Correspondence:** Email: atharqureshi469@gmail.com.

Abstract: Nano bio-MOF compounds **6**–**8** (cobalt argeninate, cobalt asparaginate, and cobalt glutaminate) have been evaluated for successful *in vitro* drugs adsorption of four drugs, terazosine, telmisartan, glimpiride and rosuvastatin. TGA and PXRD spectra of all these materials in pure form and after drugs adsorption have also been recorded to elaborate the phenomenon of *in vitro* drugs adsorption in these materials. The amounts of adsorbed drugs and their slow release from all these materials have been monitored by the high performance liquid chromatography (HPLC).

Keywords: nano bio-MOF; drugs adsorption; TGA; PXRD; HPLC

Metal Organic Frameworks (MOFs) have received over a decade's worth of attention from different aspects of significance [1,2]. Yet new areas are being explored day by day. Bio-metal organic frameworks (Bio-MOFs) are actually a subclass of MOFs [3]. These materials contain biomolecules as linkers and biocompatible metal cations as connectors [4]. MOFs can be scaled down to the nano-regime to form nanoscale metal-organic frameworks (nano-MOFs). Recently some nanoscale MOFs have been reported [5]. Although a large number of the bulk MOF materials have been synthesized and characterized up till now, but with the passage of time, the number of research reports on the nano-MOFs are also increasing day by day [6]. Nano-bio-MOFs are the nano-sized MOF materials containing biomolecules and biocompatible metal cations. This emerging class of nano-bio-MOFs can be considered as promising candidates for the drug adsorption and controlled

release due to their large surface areas, high porosity, and presence of biocompatible linker molecules [7].

Wuttke et al. have reported that MOFs materials can be designed and tuned accordingly and have been used successfully as nano-carriers with more potential compared with previously used drugs carrier materials [8–10]. Roder et al. have also reported the successful use of nano-sized MOF materials for drugs delivery. Due to their smaller size and high surface areas, these MOF materials are used as targeted drugs delivery vehicles. Several other research reports also reveal the use of nano-sized MOFs in the field of drugs delivery [11–14].

Sattar et al. [15] have reported the hydrothermal synthesis of three nano bio-MOFs compounds **6**–**8** (cobalt argeninate, cobalt asparaginate and cobalt glutaminate respectively). These compounds have been hydrothermally synthesized and characterized by Scanning Electron Microscopic (SEM) studies. Photocatalytic hydrogen production of these three compounds have been evaluated. These compounds can exhibit mulitifunctional properties. The present work comprises of the drugs adsorption studies of these three nano-bio-MOF compounds **6**–**8**. N_2 adsorption experiments of all these compounds have been recorded. *In vitro* drugs adsorption of four different drugs of all these compounds have been evaluated. Thermogravimetric analysis (TGA) and powder X-ray Diffraction Analysis (Powder XRD) patterns of all these compounds in pure form and after drugs adsorption have been recorded. The amounts of adsorbed drugs and its slow release after intervals have been monitored through the High Performance Liquid Chromatography (HPLC).

BET specific surface areas of compounds **6**, **7** and **8** have been determined as 2400 $m^2\ g^{-1}$, 2500 $m^2\ g^{-1}$ and 2200 $m^2\ g^{-1}$ respectively with a pore size of 10 Å by using BET-method based on calculations of N_2 adsorption isotherm data. Figure 1 represents the N_2 adsorption isotherm of compound **6**, **7** and **8**.

Four types of drugs (terazosine hydrochloride, telmisartan, glimpiride and rosuvastatin) have been adsorbed into compounds **6**, **7** and **8**. It was also elaborated that some pores were blocked after the drugs adsorptions thus decreasing the specific surface areas of this material as shown in Figure 1.

TGA plots of the as synthesized and drugs adsorbed compounds **6**–**8** were carried out on a SDT Q600 by heating the compounds from 0 to 600 ℃ at a heating rate of 10 ℃/min.

TGA plot of compound **6** (Figure 2a) in pure form shows first weight loss of 8% at 120 ℃ which is due to the loss of coordinated water molecule. Then up to 300 ℃ the framework shows stability with no weight loss. Second weight loss is observed at 300 ℃, which continues up to 385 ℃ with a 55% weight loss indicating the start of framework decomposition along with ligands. Then slow decomposition of framework continues gradually until the whole framework decomposes at 560 ℃ and finally the metal oxides are left. TGA plot of terazosine adsorbed compound **6** (Figure 2b) shows a weight loss of 7% at 45 ℃, which is attributed to the loss of drug molecules. At 170 ℃, the framework shows 4% weight loss which is due to the loss of coordinated water molecule. Then the framework starts to decompose. At 185 ℃ second loss of mass is observed. After that, the framework remains intact till 280 ℃, and at 285 ℃, the framework starts to decompose and this decomposition continues up to 380 ℃ with a weight loss of 58%. The whole framework decomposes along with remaining terazosine up to 590 ℃. TGA plot of telmisartan adsorbed compound **6** (Figure 2c) shows a weight loss of 5% at 40 ℃ which is due to the loss of telmisartan. At 150 ℃, a second loss of weight of 5% shows the loss of water molecules. At 250 ℃, the framework starts to

decompose which continues till 300 ℃ with a maximum weight loss of 59%. TGA plot of glimpiride adsorbed compound **6** at 25 ℃ (Figure 2d) shows first weight loss of 4% which is due to the removal of glimpiride. Then the framework remains intact up to 120 ℃, and at this temperature framework shows a weight loss of 4% up to 190 ℃ which is due to removal of coordinated water molecule. At 280 ℃, the decomposition of the framework and ligands starts which continues till 330 ℃ with weight loss of 58%. The thermogram of rosuvastatin adsorbed compound **6** (Figure 2e) shows first weight loss of 4% at 30 ℃ which is due to the removal of drug. Then the framework shows stability up to 115 ℃ and at this temperature framework shows a weight loss of 4% up to 130 ℃ which is due to removal of coordinated water molecules. After 230 ℃, the decomposition of the framework and ligands starts which continues till 555 ℃ with maximum weight loss of 58%. No further weight loss observed in the remaining range studied.

TGA plot of compound **7** in pure form (Figure 3a) shows first weight loss of 4% at 180 ℃ which is due to the loss of coordinated water molecule. Second weight loss is observed at 280 ℃ due to start of framework decomposition, which gradually and slowly continues up to 580 ℃ with a 30% loss of mass until the whole framework decomposes with the formation of metal oxides. TGA plot of terazosine adsorbed compound **7** (Figure 3b) shows a weight loss of 5% at 60 ℃, which is due to the loss of drug molecules. Then the framework shows stability up to 180 ℃. Second loss of mass at 180 ℃ is observed and this 9% weight loss is due to the loss of coordinated water molecule. After that, the framework remains intact till 280 ℃, and at 280 ℃, the framework starts to decompose and this decomposition continues up to 380 ℃ with a weight loss of 58%. The whole framework decomposes along with remaining terazosine up to 590 ℃. TGA plot of telmisartan adsorbed compound **7** (Figure 3c) shows a weight loss of 4% at 40 ℃ which is due to the loss of telmisartan. Another weight loss of 8% at 150 ℃ shows the loss of coordinated water molecule. Then the framework starts to decompose at 250 ℃ which continues till 300 ℃ with a maximum weight loss of 59%. A plot of glimpiride adsorbed compound **7** (Figure 3d) shows first weight loss of 4% at 50 ℃ which is due to the removal of glimpiride. At 170 ℃, the framework shows a weight loss of 8% up to 190 ℃ which is due to removal of water molecules. At 280 ℃, the decomposition of the framework and ligands starts which continues till 560 ℃ with weight loss of 58%. A TGA plot of rosuvastatin adsorbed compound **7** (Figure 3e) shows first weight loss of 3% at 45 ℃ which is due to the removal of drug. At 175 ℃, framework shows a weight loss of 8% up to 190 ℃ which is due to removal of water molecules. At 285 ℃, the decomposition of the framework and ligands starts which continues till 560 ℃ with weight loss of 58%. No further weight loss observed in the remaining range studied.

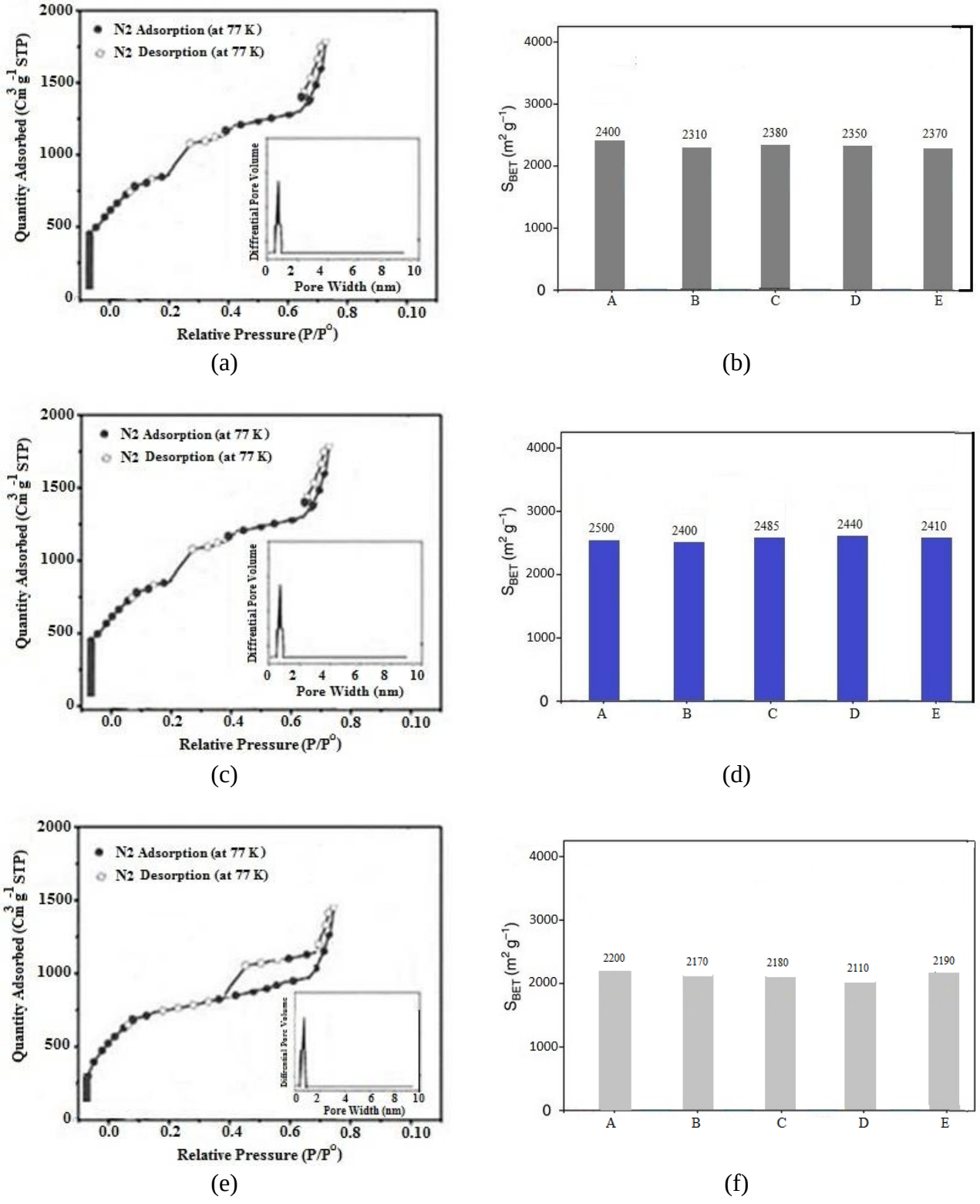

Figure 1. (a) N_2 adsorption isotherm of compound **6**, (b) BET surface area of compound **6**, (c) N_2 adsorption isotherm of compound **7**, (d) BET surface area of compound **7**, (e) N_2 adsorption isotherm of compound **8**, (f) BET surface area of compound **8** (A: Pure, B: after terazosine hydrochloride loading, C: after telmisartan loading, D: after glimpiride loading, E: after rosuvastatin loading).

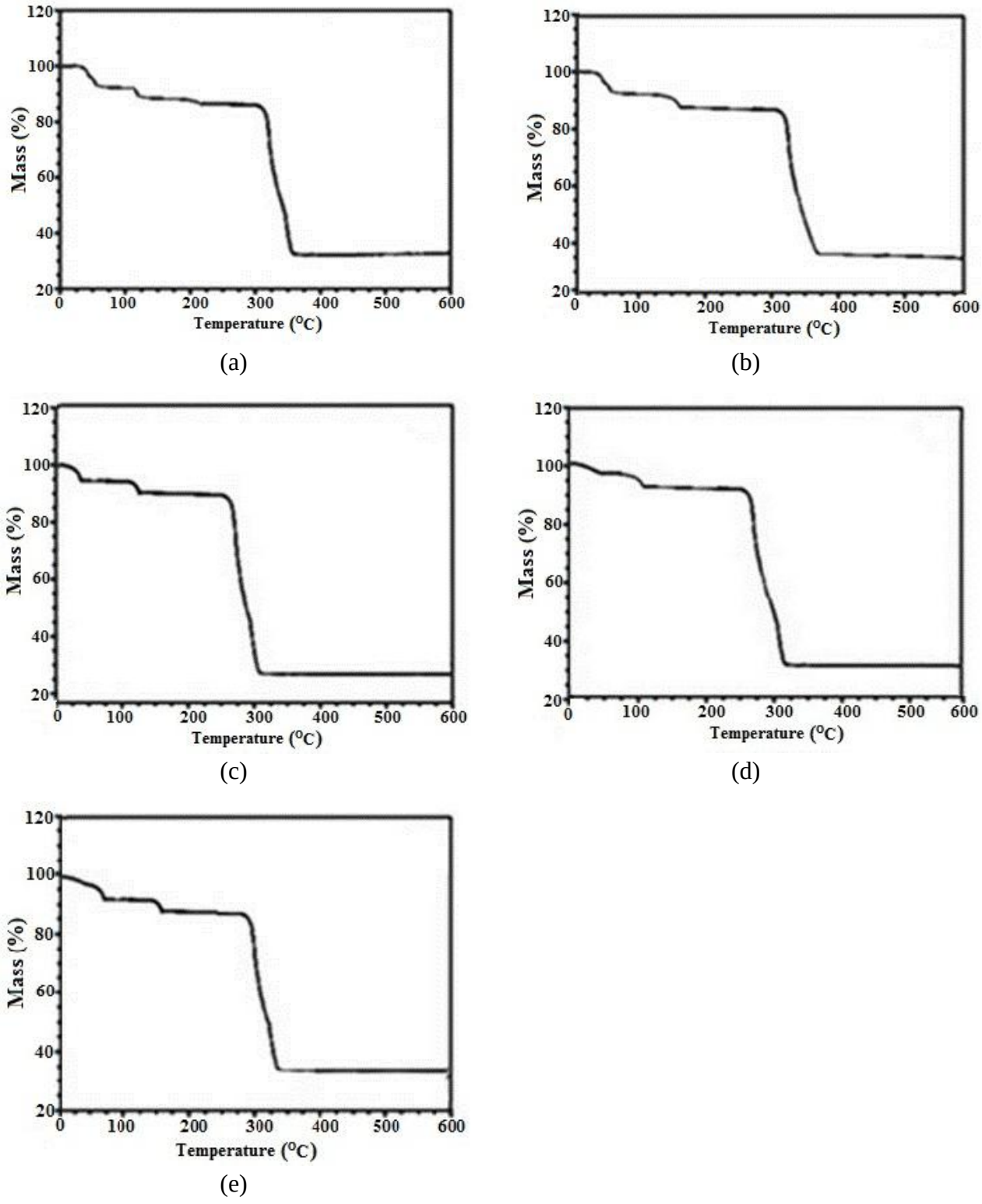

Figure 2. TGA plot of compound **6**, (a) Pure, (b) after terazosine hydrochloride loading, (c) after telmisartan loading, (d) after glimpiride loading, (e) after rosuvastatin loading.

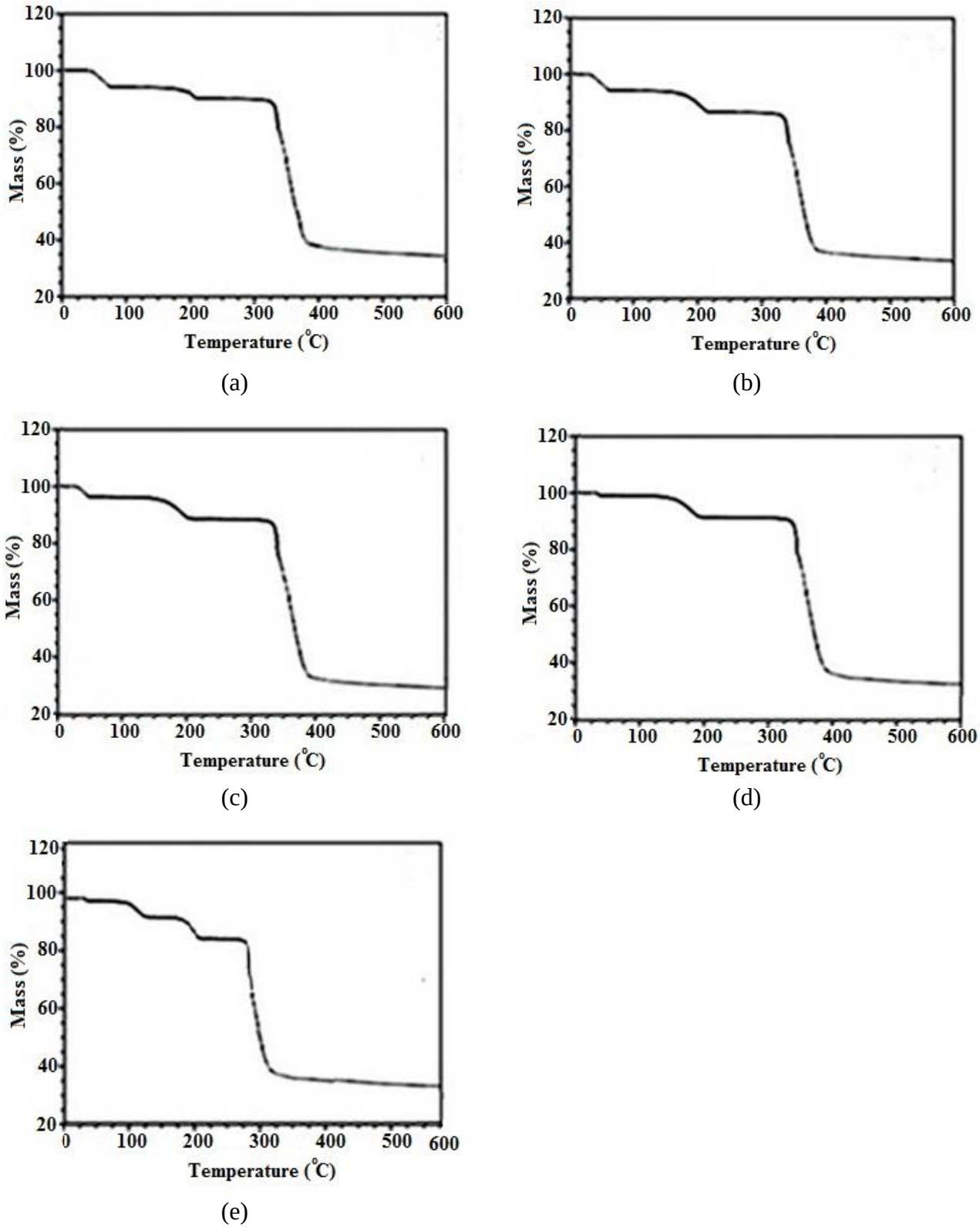

Figure 3. TGA plot of compound **7**, (a) Pure, (b) after terazosine hydrochloride loading, (c) after telmisartan loading, (d) after glimpiride loading, (e) after rosuvastatin loading.

The thermogram of compound **8** (Figure 4a) in pure form shows first weight loss of 5% at 129 ℃ which is due to the loss of water. Then up to 270 ℃, the framework remains intact, after that, the decomposition of framework starts along with ligands which continues till 320 ℃ with major weight loss of 60%. Decomposition continues gradually until 600 ℃ which weight loss of 68% shows complete decomposition of framework and formation of metal oxides. The thermogram of the terazosine loaded compound **8** (Figure 4b) indicates the first weight loss of 10% at 53 ℃ which is due to the loss of adsorbed terazosine molecules. Then up to 140 ℃, the framework shows stability, after that, weight loss of 25% can be observed up to 160 ℃ which is due to removal of water molecules. Gradual decomposition of framework and ligands starts after 300 ℃ and continues gradually till 590 ℃ with 60%. Thermogram of telmisartan loaded compound **8** (Figure 4c) indicates the first weight loss of nearly 6% at 30 ℃ which is due to the loss of adsorbed telmisartan molecules. Then up to 150 ℃, the framework shows stability, after that a weight loss of 10% is observed up to 155 ℃ which is due to the loss of coordinated water molecule. Then a gradual decomposition of framework and ligands starts which continues till 590 ℃ with maximum weight loss of 65%. While thermogram of glimpiride loaded compound **8** (Figure 4d) indicates the first weight loss of nearly 5% at 45 ℃ which is due to the loss of adsorbed glimpiride molecules. The framework shows stability for some time and at 175 ℃ the weight loss of 10% is observed which is due to the loss of coordinated water molecule. Then up to 340 ℃, the framework remains intact, after that gradual decomposition of framework and ligands starts which continues till 598 ℃ with maximum weight loss of 45%. The plot of rosuvastatin loaded compound **8** (Figure 4e) indicates the first weight loss of 4% at 50 ℃ which is due to the loss of adsorbed drug molecules. At 150 ℃, a weight loss of 8% is due to the loss of water molecules. Then up to 340 ℃, the framework remains intact, after that gradual decomposition of framework and ligands starts which continues till 556 ℃ with maximum weight loss of 50%. No further weight loss observed for the remaining range studies.

PXRD patterns of compounds **6**–**8** were recorded as described in Figure 5. Powder XRD patterns of all these new synthesized materials after drugs adsorption have revealed the permanent crystalline integrity of these compounds as these have retained its crystallinity even after soaking in water for several days.

For estimation of the drugs in the synthesized materials, High Performance Liquid Chromatography was performed on a Waters 2695 separation module. 0.139 g/g terazosine hydrochloride, 0.090 g/g telmisartan, 0.117 g/g glimpiride and 0.129 g/g rosuvastatin have been estimated in compound **6** with a maximum release time of 3, 3, 3 and 3 d respectively. 0.195 g/g terazosine, 0.055 g/g telmisartan, 0.138 g/g glimpiride and 0.095 g/g rosuvastatin were detected in compound **7**. These adsorbed amounts of drugs were slowly released from the compound after different time intervals. The maximum release time of these drugs was 5, 3, 1 and 3 d respectively. The adsorbed amounts of drugs terazosine, telmisartan, glimpiride and rosuvastatin were 0.071 g/g, 0.086 g/g, 0.135 g/g, 0.094 g/g in compound **8**. Slow release of these drugs from compound **8** was observed through HPLC. The maximum release times were 1, 3, 3 and 1 d respectively. Table 1 gives summative information about the drugs adsorption capacities of compounds **6**–**8**.

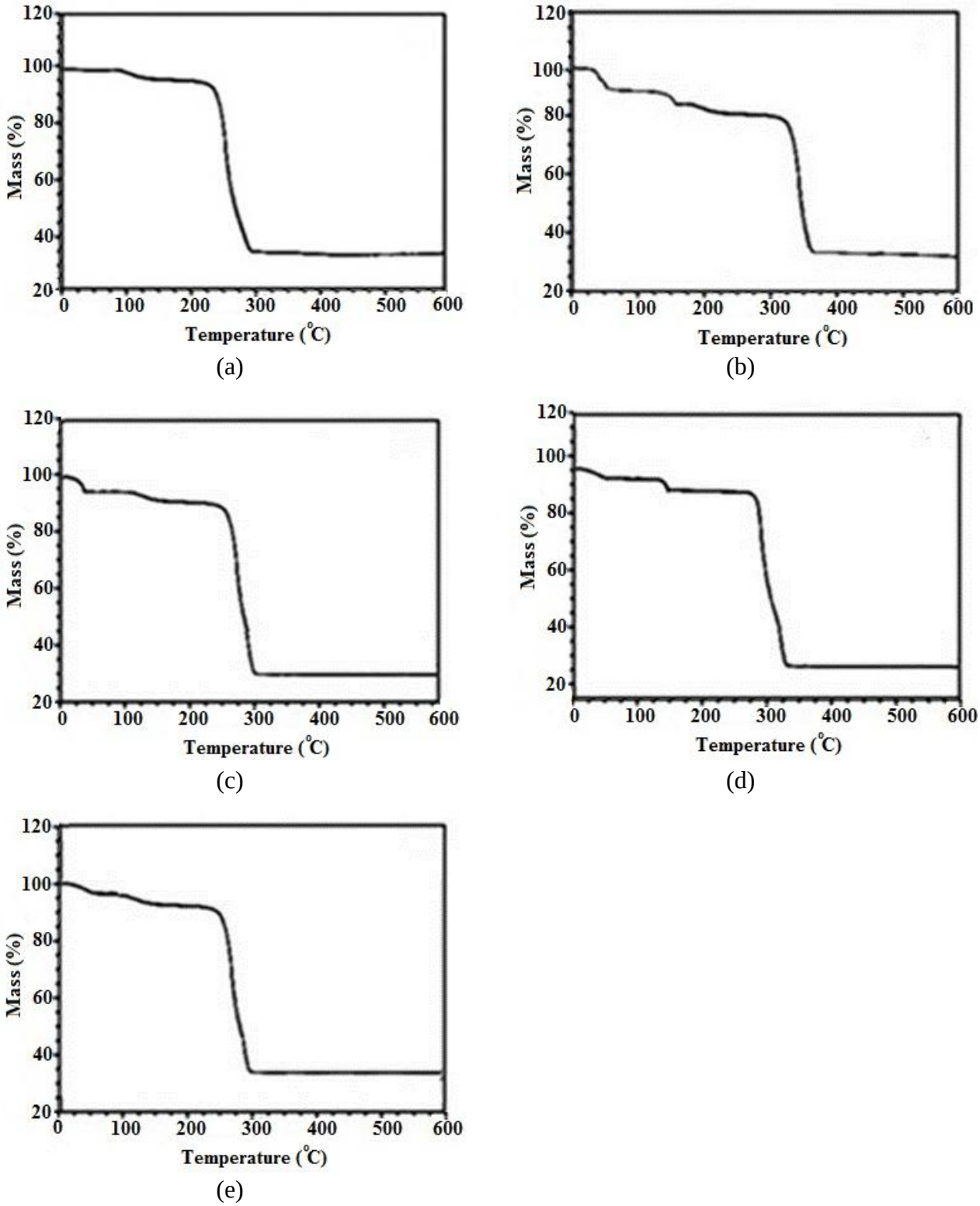

Figure 4. TGA plot of compound **8**, (a) Pure, (b) after terazosine hydrochloride loading, (c) after telmisartan loading, (d) after glimpiride loading, (e) after rosuvastatin loading.

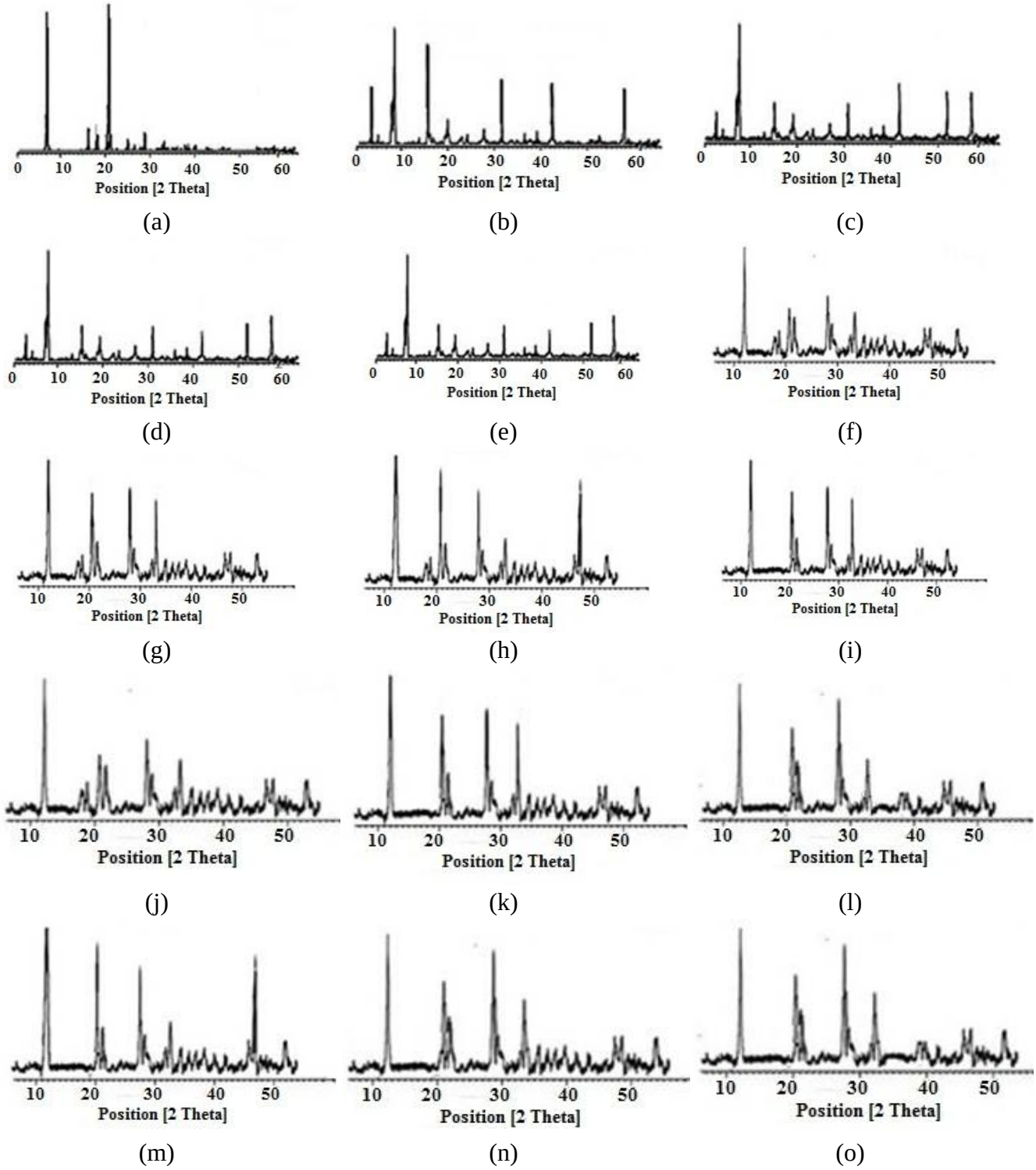

Figure 5. PXRD pattern of compound **6**, (a) Pure, (b) after terazosine hydrochloride loading, (c) after telmisartan loading, (d) after glimpiride loading, (e) after rosuvastatin loading. PXRD pattern compound **7**, (f) Pure, (g) after terazosine hydrochloride loading, (h) after telmisartan loading, (i) after glimpiride loading, (j) after rosuvastatin loading. PXRD pattern of compound **8**, (k) Pure, (l) after terazosine hydrochloride loading, (m) after telmisartan loading, (n) after glimpiride loading, (o) after rosuvastatin loading.

Table 1. A comparision of the drugs storage capacities of compounds **6**–**8.**

Synthesized porous compounds	Specific Surface areas (m^2/g)	Pore sizes (Å)	Names of drugs loaded in materials	Drugs loading capacity (%)	Time of release (days)
Compound **6**	2400	10	Terazosine hydrochloride	0.139	3
			Telmisartan	0.090	3
			Glimpiride	0.117	3
			Rosuvastatin	0.129	3
Compound **7**	2500	10	Terazosine hydrochloride	0.195	5
			Telmisartan	0.055	1
			Glimpiride	0.138	3
			Rosuvastatin	0.095	3
Compound **8**	2200	10	Terazosine hydrochloride	0.072	1
			Telmisartan	0.086	3
			Glimpiride	0.135	3
			Rosuvastatin	0.094	1

Figures in Supporting Information indicate the HPLC peaks for the estimation of adsorbed drugs in the channels of compounds **6**–**8** and their slow release after different time periods. All the details of HPLC parameters used for HPLC studies have been given in Tables S1 and S2 in Supporting Information).

In conclusion, the present work directs towards the multifunctional use of some nanosized bio-MOFs which were previously used for photocatalysis and now have been successfully utilized for the *in vitro* adsorption of terazosine, telmisartan, glimpiride and rosuvastatin drugs. This work also describes the more potential use of nanoscale bio-MOFs for drugs adsorption compared with previously used large sized carrier materials. Moreover, successful *in vitro* drug adsorption experiments on these nanosized materials will lead to their use for *in vivo* drugs adsorption as well as for the welfare of humans in medical grounds.

Conflict of interest

The authors have no conflict of interest.

References

1. Rowsell JLC, Yaghi OM (2005) Strategies for hydrogen storage in metal–organic frameworks. *Angew Chem Int Edit* 44: 4670–4679.
2. Moulton B, Zaworotko MJ (2001) From molecules to crystal engineering: supramolecular isomerism and polymorphism in network solids. *Chem Rev* 101: 1629–1658.

3. Kitagawa S, Kitaura R, Noro S (2004) Functional porous coordination polymers. *Angew Chem Int Edit* 43: 2334–2375.
4. Rieter WJ, Taylor KML, Lin W (2007) Surface modification and functionalization of nanoscale metal–organic frameworks for controlled release and luminescence sensing. *J Am Chem Soc* 129: 9852–9853.
5. Rieter WJ, Taylor KML, An H, et al. (2006) Nanoscale metal–organic frameworks as potential multimodal contrast enhancing agents. *J Am Chem Soc* 128: 9024–9025.
6. Taylor KML, Rieter WJ, Lin W (2008) Manganese-based nanoscale metal–organic frameworks for magnetic resonance imaging. *J Am Chem Soc* 130: 14358–14359.
7. Taylor KML, Jin A, Lin W (2008) Surfactant-assisted synthesis of nanoscale gadolinium metal–organic frameworks for potential multimodal imaging. *Angew Chem Int Edit* 47: 7722–7725.
8. Wuttke S, Lismont M, Escudero A, et al. (2017) Positioning metal–organic framework nanoparticles within the context of drug delivery—A comparison with mesoporous silica nanoparticles and dendrimers. *Biomaterials* 123: 172–183.
9. Lismont M, Dreesen L, Wuttke S (2017) Metal–Organic Framework Nanoparticles in Photodynamic Therapy: Current Status and Perspectives. *Adv Funct Mater* 27: 1606314.
10. He C, Liu D, Lin W (2015) Nanomedicine applications of hybrid nanomaterials built from metal–ligand coordination bonds: nanoscale metal–organic frameworks and nanoscale coordination polymers. *Chem Rev* 115: 11079–11108.
11. Röder R, Preiß T, Hirschle P, et al. (2017) Multifunctional Nanoparticles by Coordinative Self-Assembly of His-Tagged Units with Metal–Organic Frameworks. *J Am Chem Soc* 139: 2359–2368.
12. Hidalgo T, Giménez-Marqués M, Bellido E, et al. (2017) Chitosan-coated mesoporous MIL-100(Fe) nanoparticles as improved bio-compatible oral nanocarriers. *Sci Rep* 7: 43099.
13. Evans OR, Lin W (2002) Crystal engineering of NLO materials based on metal–organic coordination networks. *Accounts Chem Res* 35: 511–522.
14. Anand R, Borghi F, Manoli F, et al. (2014) Host–guest interactions in Fe (III)-trimesate MOF nanoparticles loaded with doxorubicin. *J Phys Chem B* 118: 8532–8539.
15. Sattar T, Athar M (2017) Hydrothermally Synthesized NanobioMOFs, Evaluated by Photocatalytic Hydrogen Generation. *Mod Res Catal* 6: 80–99.

AIMS Press